

Method for Determining the Absolute Number Concentration of Nanoparticles from Electrospray Sources

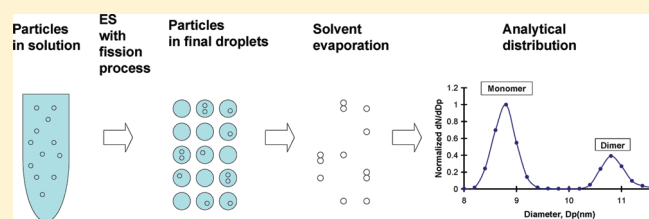
Mingdong Li,^{†,‡} Suvajyoti Guha,^{†,‡} Rebecca Zangmeister,[‡] Michael J. Tarlov,[‡] and Michael R. Zachariah^{*,†,‡}

[†]University of Maryland, College Park, Maryland 20742, United States

[‡]National Institute of Standards and Technology, Gaithersburg, Maryland 20899, United States

S Supporting Information

ABSTRACT: We have developed a simple, fast, and accurate method to measure the absolute number concentration of nanoparticles in solution. The method combines electrospray differential mobility analysis (ES-DMA) with a statistical analysis of droplet-induced oligomer formation. A key feature of the method is that it allows determination of the absolute number concentration of particles by knowing only the droplet size generated from a particular ES source, thereby eliminating the need for sample-specific calibration standards or detailed analysis



of transport losses. The approach was validated by comparing the total number concentration of monodispersed Au nanoparticles determined by ES-DMA with UV/vis measurements. We also show that this approach is valid for protein molecules by quantifying the absolute number concentration of Rituxan monoclonal antibody in solution. The methodology is applicable for quantification of any electrospray process coupled to an analytical tool that can distinguish monomers from higher order oligomers. The only requirement is that the droplet size distribution be evaluated. For users only interested in implementation of the theory, we provide a section that summarizes the relevant formulas. This method eliminates the need for sample-specific calibration standards or detailed analysis of transport losses.

1. INTRODUCTION

Nanoparticles (NPs) are finding increased use in optical sensing, diagnostics, clinical chemistry, and therapeutics. For diagnostic and therapeutic applications of NPs in humans, there will likely be strict requirements for regulatory approval such as extensive characterization of the properties of these products. In nearly all applications, one such attribute undoubtedly will be accurate determination of the particle concentration. Because of the great diversity of NPs and their associated physical and chemical properties, there currently is no one broadly applicable method for measurement of the nanoparticle concentration. For metallic nanoparticles, e.g., gold nanoparticles (Au-NPs), and protein particles, e.g., Rituxan monoclonal antibodies (Rmabs), UV/vis spectroscopy is routinely used to determine the absolute concentration in solution.^{1,2} Accurate measurement, however, requires a precise knowledge of the extinction coefficient, which depends on the particle composition, size, shape, dielectric environment, and surface coatings.^{3–6}

One of the tools we are investigating to measure the concentration of NPs involves using electrospray (ES) to generate vapor-phase-dispersed material. These aerosol materials can then be analyzed by ion mobility methods such as differential mobility analysis (DMA), also known as gas-phase electrophoretic molecular analysis (GEMMA),^{7–12} or mass spectrometry (MS) methods.^{13–17} These techniques have the potential to characterize the full size distribution and concentration of NPs in solution. However, because this is a physical sampling approach, measurements must be corrected for aerosol losses, which may depend in

an unknown way on the nature of the ES generation, ES efficiency,^{18–20} particle extraction to the DMA or MS instrument, and efficiency of particle counting instruments.

In this paper we present a new approach that exploits what is typically considered an unwanted artifact of electrospray sources, namely, droplet-induced aggregation, to extract the quantitative number concentration. By using a recently developed predictive algorithm for the measurement of the oligomer distribution in an analyte solution,²¹ we are able to quantitatively measure the number concentration of an arbitrary colloidal solution. In this paper we apply the theory given in Li et al.²¹ to obtain the absolute number concentration of the intrinsic monomer and dimer in solution. The total number concentration of monodispersed Au nanoparticles and Rmab obtained using this method in our ES-DMA work is verified by quantitative UV/vis measurement. For users only interested in implementation of the theory, we provide in section 5 a summary of relevant formulas.

2. MATERIALS AND EXPERIMENTAL METHODS

We demonstrate our approach by examining Au-NPs with an ES-DMA system described previously.²² We also show the method is applicable to biological molecules by examining Rmab to quantify the absolute number concentration of protein oligomers in solution.

Received: June 13, 2011

Revised: October 17, 2011

Published: October 27, 2011

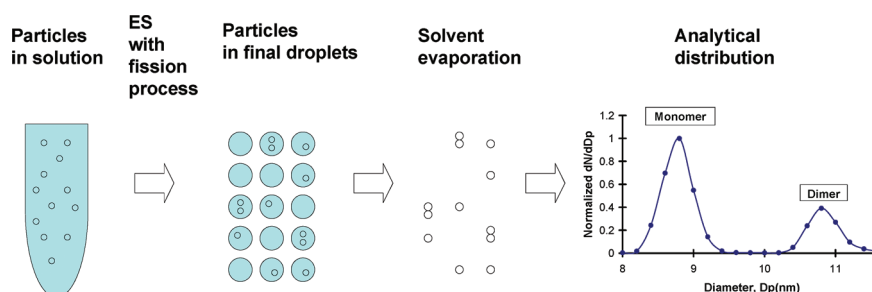


Figure 1. Schematic of the electrospray process showing the resulting measured particle size distribution observed due to droplet-induced aggregation. There are no intrinsic dimers in the original solution. However, after ES, induced dimers are observed in the analytical spectrum, and statistical analysis can be used to deduce the original monomer concentration in solution. The y -axis label “ dN/dD_p ” is defined by the total number of particles in the range $[D_p, D_p + dD_p]$ divided by the size interval, dD_p .

2.1. Gold Nanoparticle Preparation. Commercially available citrate-stabilized monodisperse Au-NPs (10 nm, 5.7×10^{12} particles/mL, Ted Pella Inc.) were used. A 1.5 mL solution of the as-received Au-NPs was centrifuged at 13 200 rpm for 45 min, and ~ 1.47 mL of the supernatant was removed and replaced with an equivalent volume of aqueous 2 mmol/L ammonium acetate solution prepared by diluting 20 mmol/L ammonium acetate at pH 10. This step was performed to remove most of the citrate stabilizer, which would otherwise coat the Au-NPs upon ES. The pH of the 20 mmol/L ammonium acetate solution was adjusted by addition of ammonium hydroxide. The solution was then centrifuged again for 15 min, and 1.4 mL of supernatant was removed to obtain a highly concentrated Au-NP sample. The number concentration of Au-NPs in 1.4 mL of supernatant, C_w , was measured by UV/vis spectroscopy by comparison of the peak absorbance value of the supernatant solution with that of the as-received Au-NPs of known concentration at a wavelength of ~ 520 nm. Four replicate Au-NP samples were prepared following the protocol described above and are noted as samples 1–4. The as-prepared Au-NP samples were then electrosprayed into the DMA–condensation particle counter (CPC) system after $2\times$, $4\times$, or $8\times$ dilution with 2 mmol/L ammonium acetate solution.

2.2. Rmab Solution Preparation. Formulated Rmab (145 kDa) was purified using a protein A affinity column. Purified Rmab was stored at -18°C in 25 mmol/L Tris buffer, pH 7.4, with 0.01% sodium azide (NaN_3) added as a preservative. Immediately prior to use in ES studies, the storage buffer was exchanged for 20 mmol/L ammonium acetate, pH 7, by washing all salts from Rmab using a centrifugal filter device with a mass cutoff of 30 kDa. The concentration of Rmab in 20 mmol/L ammonium acetate was adjusted to 1 mg/mL as verified by measuring the maximum absorbance at 280 nm and using a molar absorptivity of $236\,020\ (\text{mol/L})^{-1}\ \text{cm}^{-1}$. Working solutions of 100, 50, 25, 10, and 5 $\mu\text{g/mL}$ concentrations were made by dilution with 20 mmol/L ammonium acetate and used for ES studies.

2.3. Electrospray Particle Generation and Differential Mobility Measurements. Aerosolized droplets were generated using a $40\ \mu\text{m}$ inner diameter capillary for Au-NP samples and a $25\ \mu\text{m}$ inner diameter capillary for Rmab mounted in an electrospray aerosol generator (model 3480, TSI Inc.) where the liquid flow rates through the capillaries were ~ 433 and ~ 66 nL/min, respectively.²³ The ES generator was operated with a carrier gas of 1 L/min of purified air and 0.2 L/min of carbon dioxide to stabilize the Taylor cone. A stable Taylor cone is necessary to quantitatively determine droplet-induced aggregation and the absolute particle number concentration. The aerosolized droplets are then passed over a radioactive Po-210(α) source that reduces the charge on the droplets to a well-defined Boltzmann equilibrium charge distribution.²⁴ With this known charge distribution, the total number of particles can be obtained by counting the number of single positively charged particles. The neutralized dry particles entered a differential mobility analyzer (model 3485 Nano DMA

column, TSI Inc.) for particle size measurement and were subsequently counted with an ultrafine CPC (model 3025A, TSI Inc.). The differential mobility analyzer consists of a grounded cylinder and an inner negative high voltage rod with a slit for the particles of given mobility size to exit and be counted by the CPC. By scanning the center rod voltage, different size particles can be extracted to build a size distribution for a given particle population. Unlike a mass spectrometer, which selects particles on the basis of the mass/charge ratio, the differential mobility analyzer selects particles on the basis of their equivalent mobility diameters. In the simplest case, i.e., particles in the free molecule regime, the mobility scales with the inverse of the projected area to charge ratio. The size-selection resolution of the DMA instrument is determined by the ratio of sheath to aerosol flow rates within the DMA instrument. To achieve sufficient resolution in our experiment, the nano differential mobility analyzer was operated with a sheath flow of 30 L/min and an aerosol flow of 1.2 L/min, which enables an operating range of between 2 and 45 nm. For our operating conditions we have found a lower number concentration limit of $\sim 10^9$ particles/ cm^3 for particles of <100 nm. A different choice of flow rates and the use of a different length DMA instrument would enable a different size range to be classified. Because this is an ion mobility measurement, the composition of the analyte particle is not relevant to the operational principles of the instrument. More details on the measurement method can be found in the paper by Tsai et al.²²

2.4. Droplet Size Measurements. To employ our method for quantification, knowledge of the droplet size generated by the ES source is required. The statistical analysis of droplet-induced aggregation requires a droplet size distribution. Further explanations are shown in the Supporting Information. The droplet size distribution was determined by electrospraying a known concentration (v/v) of sucrose solution and measuring the resultant dry particle size distribution. Using this procedure, the droplet size distribution can be determined directly. For droplet size evaluation, sucrose solution concentrations of 0.0315% and of 0.063% (v/v) were used for Au-NP and Rmab measurements, respectively. At such low concentrations of sucrose and analytes, the viscosity of the solutions is governed by the buffer conditions, and the droplet size of these solutions can be evaluated by^{23,25}

$$D_d = \frac{1}{C_s^{1/3}} D_s \quad (1)$$

where D_d is the droplet diameter, D_s is the sucrose particle diameter after drying (measured by DMA), and C_s is the sucrose concentration (v/v) in the ES solution.

3. THEORY OF DETERMINING THE ABSOLUTE NUMBER CONCENTRATION

In the oligomer distribution study of Li et al.,²¹ unintentional (nonspecific) analyte aggregation in electrospray sampling,

called droplet-induced aggregation, was addressed and quantified. In any electrospray process, induced aggregation within a droplet can be a confounding artifact to prediction of the true oligomer distribution in solution. However, we have found that this effect can be a very useful probe to directly deduce the monomer concentration in solution without the need to calibrate the losses of the ES process and the losses postelectrospray. To explain this clearly, we first describe the electrospray process and introduce the effect of droplet-induced aggregation. The mechanism of ES has been treated in great detail by Kebarle et al.²⁶ and Gaskell²⁷ as well as others. In ES, the application of a high voltage to a capillary will induce, due to Coulombic repulsion, small droplet formation. It is well accepted that large and compact multiply charged ions, which are the analytes of interest in this work, are produced as charged residues after complete drop evaporation after serial fission processes.²⁸ Evaporation of the solvent leaves behind the analyte (e.g., protein, particle, virus, etc.), which is then passed to an analyzer such as a differential mobility analyzer or mass spectrometer. When two or more analyte molecules or particles exist in a final droplet, and the droplet eventually dries, oligomers are observed in the MS or DMA spectrum (Figure 1). We recently investigated this effect through a statistical model by Li et al.²¹ that allowed us to separate the true oligomer concentration from the induced concentration. In this work we extend the analysis to use the induced oligomer formation to extract the absolute number concentrations of monomers and oligomers in solution.

3.1. Physical Aggregation (Droplet-Induced Aggregation) of Particles. In an electrospray of a colloid there is a finite probability, depending on the particle concentration and droplet size, that more than one particle will be within a droplet. Upon evaporation of the solvent, aggregation of the particles is induced. If a final droplet generated in an ES after a series of fission processes is a random sample of the solution, the size of a droplet is much greater than the size of the particles, and the oligomer particles in the solution are random and independent, then the distribution of observed oligomers in droplets can be quantitatively described.²¹ Here we first introduce a theory in general form describing the full droplet size distribution, and then we derive two approximations under two different limiting cases and apply them to obtain the absolute number concentrations of monomers and dimers in solution. The essential feature of this approach is that the observed dimer/monomer ratio is a unique function of the droplet size and the initial monomer concentration. This same strategy can also be expanded to quantify the absolute concentrations of any higher order aggregates. Below we derive working relationships for some useful cases.

3.2. Droplet-Induced Aggregation of Identical Particles (Monomers) from Droplets of Identical Size Generated by ES. If a final droplet generated in ES after the fission process is a random sample of the solution and the particles in the solution are identical and exist only as monomers, the probability that there are k particles in a given droplet obeys a Poisson distribution^{7,21,29} and is given by

$$P(k, \lambda) = \frac{e^{-\lambda} \lambda^k}{k!} \quad (2)$$

where λ is the mean number of particles per droplet and is given by

$$\lambda = V_d C_p = \frac{1}{6} \pi D_d^3 C_p \quad (3)$$

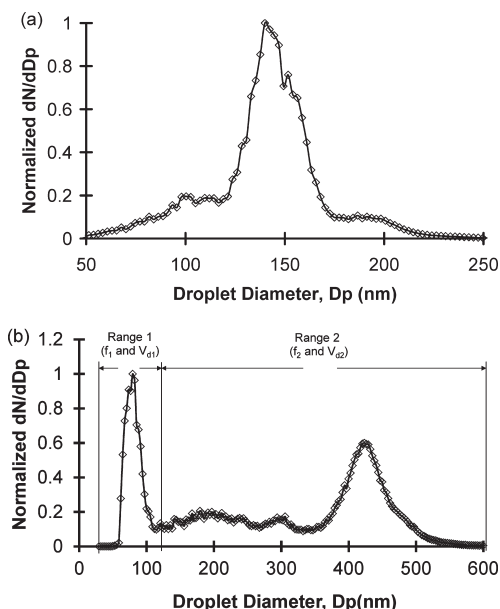


Figure 2. (a) ES monomodal and narrow droplet size distribution measured from sucrose at 20 mmol of ammonium acetate buffer (section 2.4) and used for Rmab samples at the same buffer condition in section 4.1.2. (b) ES droplet with a bimodal size distribution measured from sucrose at 2 mmol of ammonium acetate buffer (section 2.4) and used for Au-NP samples 3 and 4 in section 4.1.1. The y-axis label “ dN/dD_p ” is defined by the total number of particles in the range $[D_p, D_p + dD_p]$ divided by the size interval, dD_p .

where V_d is the final droplet volume, D_d is the final droplet diameter, and C_p is the number concentration of the particles in solution.

3.3. Droplet-Induced Aggregation of Monomers and Dimers in Solution from Droplets: General Case. If we consider an arbitrary droplet size distribution, $f(D_d)$, from an ES source and assume intrinsic monomers and dimers in solution, a general relationship for the observed dimer to monomer ratio is given by²¹

$$\frac{N_{o2}}{N_{o1}} = \frac{\int f(D_d) P_2 dD_d}{\int f(D_d) P_1 dD_d} \quad (4)$$

where

$$\int f(D_d) dD_d = 1$$

$$P_1 = e^{-(\lambda_1 + \lambda_2)} \lambda_1 \quad (5)$$

is the probability of monomers observed in the final droplet with diameter D_d

$$P_2 = e^{-(\lambda_1 + \lambda_2)} \left(\frac{\lambda_1^2}{2} + \lambda_2 \right) \quad (6)$$

is the probability of dimers observed in the final droplet with diameter D_d , $\lambda_1 = V_d C_{p1} = \frac{1}{6} \pi D_d^3 C_{p1}$ is the mean number of monomers per droplet, $\lambda_2 = V_d C_{p2} = \frac{1}{6} \pi D_d^3 C_{p2}$ is the mean number of dimers per droplet, V_d is the final droplet volume, and D_d is the final droplet diameter. Here the number

concentration of intrinsic monomers in solution is C_{p1} , and the number concentration of intrinsic dimers in solution is C_{p2} . Then following electrospray, we observe N_{o1} monomers and N_{o2} dimers.

Equations 5 and 6 were obtained assuming that the size of a droplet is much greater than the size of the analyte particles and that the partial spatial distributions are independent of each other; i.e., oligomers in the ES process follow an independent joint Poisson distribution. A more accurate form of (P_1, P_2) can be obtained using the methodology we have previously described in the statistical online Supporting Information for the paper by Li et al.²¹ In this work we use eqs 5 and 6.

Although it is difficult to solve eq 4 for C_{p1} and C_{p2} directly, accurate approximations can be obtained under some limiting conditions.

3.3.1. Monomodal and Narrow Droplet Size Distribution. For the first limiting condition, the droplet size distribution $f(D_d)$ is considered to be monomodal and relatively narrow. As an example, we consider in Figure 2a a droplet size distribution from ES measured for sucrose in 20 mmol/L ammonium acetate. In this case eq 4 can be evaluated with one average droplet volume:²¹

$$\frac{N_{o2}}{N_{o1}} \approx \frac{P_2|_{V_d=\bar{V}_d}}{P_1|_{V_d=\bar{V}_d}} = \frac{\bar{V}_d C_{p1}}{2} + \frac{C_{p2}}{C_{p1}} \quad (7)$$

where

$$\bar{V}_d = \sum_i f(D_{d,i}) V_{d,i} = \sum_i f(D_{d,i}) \frac{1}{6} \pi D_{d,i}^3 \quad (8)$$

$$\sum_i f(D_{d,i}) = 1$$

3.3.2. Bimodal Droplet Size Distribution $f(D_d)$. If the size distribution $f(D_d)$ is bimodal as, for example, shown in Figure 2b, then eq 4 can be approximated by using two average droplet volumes, \bar{V}_{d1} in range 1 and \bar{V}_{d2} in range 2. If the concentrations are not very high, that is, $\bar{V}_{d2}(C_{p1} + C_{p2})$ is not much greater than unity, eq 4 can be further approximated by using only one average droplet volume, \bar{V}_{d2} :

$$\frac{N_{o2}}{N_{o1}} \approx \frac{\bar{V}_{d2} C_{p1}}{2} + \frac{C_{p2}}{C_{p1}} \quad (9)$$

The derivations and more approximated formulas in these two limiting cases are shown in the Supporting Information.

Thus, from a measurement of the “observed” monomers and dimers (N_{o1} , N_{o2}), the absolute number concentration of intrinsic monomers, C_{p1} , can be obtained through evaluation of eq 4 directly or through its accurate approximations (eqs 7 and 9) under the appropriate conditions described above. The only requirement for this method is that the final droplet size distribution be determined, which can be done in the absence of analyte as described above in section 2.4. Thus, this method eliminates the need for sample-specific calibration standards or detailed analysis of transport losses.

4. RESULTS AND DISCUSSION

We describe two approaches for making absolute concentration measurements and apply them to nanoparticles and protein: (1) determination of the absolute number concentration by serial

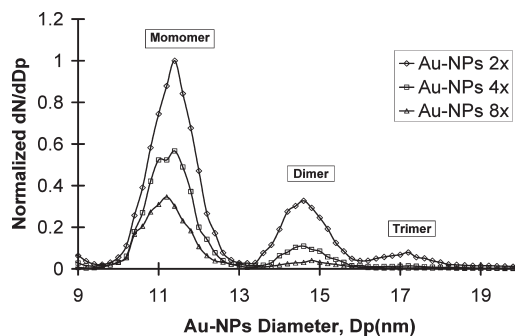


Figure 3. ES-DMA size distributions of 10 nm Au-NPs, sample 4. The rhombus, square, and triangle data markers are those of 2×, 4×, and 8× dilutions of the original sample, respectively. Each of the discernible oligomer peaks are labeled. The y-axis label “ dN/dD_p ” is defined by the total number of particles in the range $[D_p, D_p + dD_p]$ divided by the size interval, dD_p .

dilution and (2) determination of the absolute number concentration by changing the droplet size.

4.1. Determination of the Absolute Number Concentrations by Serial Dilution. **4.1.1. Absolute Number Concentrations of Au-NPs.** In this section we discuss how, following an experimental strategy based on the relationship derived in the theory section, we can determine the absolute number concentrations of NPs in solution.

Figure 2b shows the droplet size distribution measured from sucrose solution in 2 mmol/L ammonium acetate buffer and the identical buffer solution used for Au-NP samples. On the basis of the distribution in Figure 2b and the bimodal droplet size approximation, the absolute number concentrations of monomers and dimers of Au-NPs can be obtained by a series of measurements at various dilutions for irreversible aggregation:

$$C_{p1} = \frac{4}{\bar{V}_{d2}} \left(\frac{N_{o2}}{N_{o1}} - \frac{N_{o2,2x}}{N_{o1,2x}} \right) \quad (10)$$

$$C_{p2} = \frac{4}{\bar{V}_{d2}} \left(\frac{N_{o2}}{N_{o1}} - \frac{N_{o2,2x}}{N_{o1,2x}} \right) \left(2 \frac{N_{o2,2x}}{N_{o1,2x}} - \frac{N_{o2}}{N_{o1}} \right) \quad (11)$$

where $N_{o1,2x}$ is the observed number of monomers after 2× dilution and $N_{o2,2x}$ is the observed number of dimers after 2× dilution. The detailed derivation is shown in the Supporting Information.

Figure 3 shows the observed size distribution for 2×, 4×, and 8× dilutions of 10 nm Au-NPs (sample 4). Using the data, we can evaluate eqs 10 and 11 to determine the absolute concentrations in solution.

It would be best to use an orthogonal method to ascertain the validity of our measurement and data analysis approach, but an independent measure of both the monomer and dimer concentrations is unavailable. We can, however, compare the sum of our monomer and dimer measurements with the total number concentration of Au-NPs provided by the vendor and independent UV/vis measurements.

Table 1 shows the intrinsic number concentrations for the 1× Au-NP samples based on the observed numbers of monomers and dimers measured with ES-DMA at 2×, 4×, and 8× dilutions for Au-NP samples 1–4 using eqs 10 and 11. For each sample, the total number concentration of monomers, whether

Table 1. Comparison of ES-DMA-Measured Concentrations for the 1× Au-NP Samples and Those from UV/Vis of Au-NPs (Samples 1–4)^a

expt number	based on Au-NPs at	ES-DMA—CPC-observed results + droplet-induced	
		model (number/mL), $C_{p1} + 2C_{p2}$	UV/vis measurement (number/mL), $C_{UV/vis}$
1	2× and 4× dilutions of sample 1	5.20×10^{13}	4.81×10^{13}
2	4× and 8× dilutions of sample 1	4.02×10^{13}	4.81×10^{13}
3	2× and 4× dilutions of sample 2	5.07×10^{13}	5.15×10^{13}
4	4× and 8× dilutions of sample 2	4.18×10^{13}	5.15×10^{13}
5	2× and 4× dilutions of sample 3	4.59×10^{13}	4.92×10^{13}
6	4× and 8× dilutions of sample 3	4.51×10^{13}	4.92×10^{13}
7	2× and 4× dilutions of sample 4	5.15×10^{13}	5.01×10^{13}
8	4× and 8× dilutions of sample 4	4.50×10^{13}	5.01×10^{13}

^aFor each sample, the total number concentration of monomers whether free or aggregated, $C_{p1} + 2C_{p2}$, is calculated and compared with the total number concentration obtained from UV/vis and supplier specification.

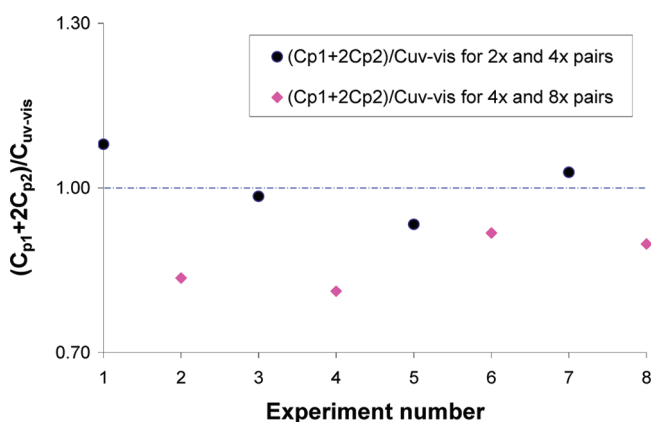


Figure 4. The total number concentration of monomers whether free or aggregated, $C_{p1} + 2C_{p2}$, calculated on the basis of eqs 10 and 11 is divided by the total number concentration $C_{UV/vis}$ obtained from UV/vis and vendor specification. The x -axis is the experiment index number. The circle and rhombus symbols are those for 2× and 4× dilution pairs and for 4× and 8× dilution pairs, respectively. Lower dilution pairs (solid circles) provide more accurate results.

free or aggregated, $C_{p1} + 2C_{p2}$, is calculated and compared with the total number concentration obtained from UV/vis and the vendor's specification.

Another way to view these results is presented in Figure 4, which plots the ES-DMA to UV/vis measurement as a function of the experiment number. To compare clearly the results from the two measurement methods above, the $C_{p1} + 2C_{p2}$ values (from the droplet-induced model) are normalized by $C_{UV/vis}$ (obtained from the UV/vis measurements and the vendor specification) and displayed in Figure 4 as a function of the experiment number.

These results show good agreement for the low-dilution pairs and poorer agreement for the high-dilution pairs. The normalized value of $C_{p1} + 2C_{p2}$ is 1.01 ± 0.05 for low-dilution pairs and 0.87 ± 0.04 for high-dilution pairs. The calculations are based on bimodal droplet size approximation using eqs 10 and 11. The discrepancy between them can likely be attributed to the fact that the distribution in Figure 2b is not truly bimodal (i.e., note the satellite peaks). However, overall the method as outlined above allows a simple and reasonably accurate determination of the particle concentration without the need for calibration of the ES source or detector (CPC–DMA).

4.1.2. Determination of Absolute Number Concentrations of Rmab Protein by Serial Dilution. A serial dilution of the Rmab sample was prepared with concentrations of 100 $\mu\text{g/mL}$ (1×), 50 $\mu\text{g/mL}$ (2×), 25 $\mu\text{g/mL}$ (4×), 10 $\mu\text{g/mL}$ (10×), and 5 $\mu\text{g/mL}$ (20×) at pH 7 in 20 mmol/L ammonium acetate buffer. The dilution method described in section 4.1.1 was then used to estimate the total number concentration of monomers whether free or aggregated, $C_{p1} + 2C_{p2}$, of the 1× sample, and this value was compared to the known concentration, 100 $\mu\text{g/mL}$.

Figure 2a shows the droplet size distribution under the same experimental conditions. The distribution is monomodal. Using the dilution method described in section 4.1.1, the total number concentrations of monomers whether free or aggregated of the 1× sample, $C_{p1} + 2C_{p2}$, are calculated and shown in Table 2.

Examination of Table 2 shows that the total number concentration calculated from the droplet-induced model is $107.3 \pm 3.3 \mu\text{g/mL}$, which compares reasonably with the known value of 100 $\mu\text{g/mL}$.

The determination of the absolute number concentration by serial dilution is expected only for irreversible aggregations. However, because the intrinsic dimer concentrations in Au-NP and Rmab protein samples under the conditions in this work are at most 5% on the basis of the work of Li et al.,²¹ i.e., essentially only monomers exist in solution, the serial dilution method can be used for both Au-NPs and Rmab protein.

4.2. Determination of the Absolute Number Concentration by Changing the Droplet Size: Application to Measurement of Rmab Protein. In this section we show another experimental strategy using a series of measurements under different droplet size distributions to measure the concentration of biological molecules, in this case the Rmab protein. This strategy can be used for both reversible and irreversible aggregation.

The ES droplet size distribution was changed by varying the chamber pressure across the capillary in the electrospray source. Figure 5a shows the droplet size distributions from sucrose solution at pH 7 in 20 mmol/L ammonium acetate buffer with chamber pressures of 3.0 psi (20 700 Pa) and 3.7 psi (25 500 Pa). Figure 5b shows the observed size distributions of Rmab at a concentration of 100 $\mu\text{g/mL}$ in the same buffer. On the basis of the droplet size distributions in Figure 5a, the average droplet volumes are calculated and shown in Table 3. Because the droplet size distributions in Figure 5a are monomodal, the monomodal droplet size approximation is used and the intrinsic number

Table 2. Total Number Concentrations of Monomers Whether Free or Aggregated of the 1 × Rituxan Sample, $C_{p1} + 2C_{p2}$, Calculated on the Basis of the Observed Numbers of Monomers and Dimers Measured with ES-DMA–CPC at Various Dilutions at pH 7 in 20 mmol/L Ammonium Acetate Buffer and the Dilution Method, eqs 13 and 14^a

expt number	ES-DMA results + droplet-induced model		
	Rmab at	measured ($\mu\text{g/mL}$)	known conc, C_p ($\mu\text{g/mL}$)
1	100 and 50 $\mu\text{g/mL}$	110	100
2	50 and 25 $\mu\text{g/mL}$	111	100
3	25 and 10 $\mu\text{g/mL}$	104	100
4	10 and 5 $\mu\text{g/mL}$	104	100

^aThe values then are compared with the known total number concentration, 100 $\mu\text{g/mL}$.

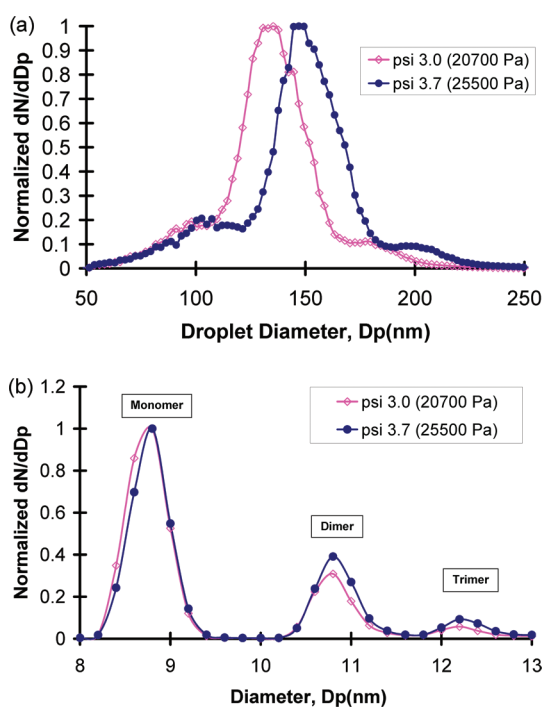


Figure 5. (a) ES droplet size distributions measured from sucrose at pH 7 in 20 mmol/L ammonium acetate buffer (section 2.4) at pressures of 3.0 psi (2.07×10^4 Pa) (open symbols) and 3.7 psi (2.55×10^4 Pa) (closed symbols). (b) Observed ES-DMA size distributions of Rmab at pH 7 in 20 mmol/L ammonium acetate buffer at chamber pressures of 3.0 psi (2.07×10^4 Pa) (open symbols) and 3.7 psi (2.55×10^4 Pa) (closed symbols). Each of the discernible oligomer peaks are labeled. The y-axis label “ dN/dD_p ” is defined by the total number of particles in the range $[D_p, D_p + dD_p]$ divided by the size interval, dD_p .

concentrations of monomers and dimers of Rmab, C_{p1} and C_{p2} , can be obtained from the following equations:

$$\frac{N_{o2}}{N_{o1}} = \frac{\bar{V}_d C_{p1}}{2} + \frac{C_{p2}}{C_{p1}} \quad (7)$$

$$\frac{N_{o2, \bar{V}_d'}}{N_{o1, \bar{V}_d'}} = \frac{\bar{V}_d' C_{p1}}{2} + \frac{C_{p2}}{C_{p1}} \quad (12)$$

where N_{o1} and N_{o2} are the observed numbers of monomers and dimers, respectively, at the average droplet volume \bar{V}_d , while $N_{o1, \bar{V}_d'}$ and $N_{o2, \bar{V}_d'}$ are the observed numbers of monomers and dimers, respectively, at the average droplet volume \bar{V}_d' . The detailed derivation of eqs 7 and 12 is shown in the Supporting Information.

Table 3 shows the ratios of observed dimers to monomers for Rmab measured in ES-DMA experiments at a concentration of 100 $\mu\text{g/mL}$ at pH 7 and with ES chamber pressures of 3.0 psi (2.07×10^4 Pa) and 3.7 psi (2.55×10^4 Pa). For each experiment, the total number concentration of monomers whether free or aggregated, $C_{p1} + 2C_{p2}$, is calculated on the basis of eqs 7 and 12 and compared with the known concentration of 100 $\mu\text{g/mL}$. Experiments were repeated twice with two different capillaries (cap 1 and cap 2) of nominally identical size.

The results presented in Table 3 show that the total absolute number concentrations, $C_{p1} + 2C_{p2}$, calculated from our droplet-induced model are in reasonable agreement with the known concentration.

We have shown that two approaches, serial dilution and varying the droplet size, can be used to determine the absolute number concentration without the need for standards or system calibration as long as the ES droplet size can be determined. We believe, however, that the approach of varying the droplet size is a more general method because serial dilution is valid only for irreversible aggregating systems.

5. SUMMARY OF LIMITING CASES AND CORRESPONDING FORMULAS

In this section, each limiting case and the relevant formula are listed.

Definitions:

- $f(D_d)$ = droplet size distribution, which can be measured experimentally from sucrose solution under the same buffer conditions (section 2.4)
- D_d = droplet diameter
- \bar{V}_d = average droplet volume as determined from $f(D_d)$
- N_{o1} = observed number of monomers after electrospray
- N_{o2} = observed number of dimers after electrospray
- $N_{o1, 2\times}$ = observed number of monomers after 2× dilution
- $N_{o2, 2\times}$ = observed number of dimers after 2× dilution
- C_{p1} = number concentration of monomers in original solution
- C_{p2} = number concentration of dimers in original solution

5.1. Monomodal and Narrow Droplet Size Distribution, $f(D_d)$: Method. 5.1.1. Absolute Number Concentrations by Serial Dilution (Irreversible Aggregation): $\bar{V}_d(C_{p1} + C_{p2}) \leq 1$. The intrinsic number concentrations of monomers and dimers are

$$C_{p1} \approx \frac{4}{\bar{V}_d} \left(\frac{N_{o2}}{N_{o1}} - \frac{N_{o2, 2\times}}{N_{o1, 2\times}} \right) \quad (13)$$

$$C_{p2} \approx \frac{4}{\bar{V}_d} \left(\frac{N_{o2}}{N_{o1}} - \frac{N_{o2, 2\times}}{N_{o1, 2\times}} \right) \left(2 \frac{N_{o2, 2\times}}{N_{o1, 2\times}} - \frac{N_{o2}}{N_{o1}} \right) \quad (14)$$

5.1.2. Absolute Number Concentrations by Changing the droplet Size (Irreversible/Reversible): $\bar{V}_d(C_{p1} + C_{p2}) \leq 1$. The intrinsic number concentrations of monomers and dimers,

Table 3. Ratios of Observed Dimers to Monomers for Rmab Measured in ES-DMA Experiments at pH 7 and at a Concentration of 100 $\mu\text{g}/\text{mL}$ with the Chamber Pressures in ES at 3.0 psi (2.07×10^4 Pa) and 3.7 psi (2.55×10^4 Pa)^a

exp index	3.7 psi (2.55×10^4 Pa)		3.0 psi (2.07×10^4 Pa)		$C_{p1} + 2C_{p2}$ from droplet-induced theory		
	obsd dimer to monomer ratio (%)	average droplet volume (m^3)	obsd dimer to monomer ratio (%)	average droplet volume (m^3)	number/mL	$\mu\text{g}/\text{mL}$	known concentration C_p ($\mu\text{g}/\text{mL}$)
cap 1	37.4	1.64×10^{-21}	29.5	1.22×10^{-21}	4.24×10^{14}	102.2	100
cap 2	40.6	1.84×10^{-21}	31.0	1.38×10^{-21}	4.26×10^{14}	105.7	100

^a For each experiment, the total number concentration of monomers whether free or aggregated, $C_{p1} + 2C_{p2}$, is calculated on the basis of eqs 7 and 12 and compared with the known total concentration, 100 $\mu\text{g}/\text{mL}$.

C_{p1} and C_{p2} , can be obtained from the following equations:

$$\frac{N_{o2}}{N_{o1}} \approx \frac{\bar{V}_d' C_{p1}}{2} + \frac{C_{p2}}{C_{p1}} \quad (7)$$

$$\frac{N_{o2, \bar{V}_d'}}{N_{o1, \bar{V}_d'}} \approx \frac{\bar{V}_d' C_{p1}}{2} + \frac{C_{p2}}{C_{p1}} \quad (12)$$

where $N_{o1, \bar{V}_d'}$ and $N_{o2, \bar{V}_d'}$ are the observed numbers of monomers and dimers, respectively, at the average droplet volume \bar{V}_d' .

5.2. Bimodal Droplet Size Distribution, $f(D_d)$: Method.
5.2.1. Absolute Number Concentrations by Serial Dilution (Irreversible Aggregation): $\bar{V}_{d2}(C_{p1} + C_{p2}) \leq 1$. The intrinsic number concentrations of monomers and dimers can be obtained from eqs 13 and 14 by replacing \bar{V}_d with \bar{V}_{d2} , the average droplet volume within range 2 (see Figure 2b), in both equations.

5.2.2. Absolute Number Concentrations by Changing the Droplet Size (Irreversible/Reversible): $\bar{V}_{d2}(C_{p1} + C_{p2}) \leq 1$. The intrinsic number concentrations of monomers and dimers, C_{p1} and C_{p2} , can be obtained from eqs 7 and 12 by replacing \bar{V}_d with \bar{V}_{d2} , the average droplet volume within range 2 (see Figure 2b) in eq 7, and by replacing \bar{V}_d' with \bar{V}_{d2}' , the other average droplet volume within range 2 (see Figure 2b), in eq 12.

6. CONCLUSIONS

We have developed a simple, fast, and accurate method to measure the absolute number concentration of nanoparticles in solution from electrospray by understanding the statistical basis of induced oligomer formation during electrospray. We first introduced the droplet-induced aggregation theory given in the paper by Li et al.²¹ in a general form and then applied it to obtain the absolute number concentration of intrinsic monomers and dimers in solution using ES-DMA. The total number concentration of monodispersed Au nanoparticles obtained using this method was verified by UV/vis measurements. We also showed the approach is applicable to biological molecules by measuring the concentration of Rmab. We believe the methodology can be used with any electrospray process coupled to an analytical tool that can distinguish monomers from higher order oligomers. The only requirement is that the droplet size distribution be determined. The real power of the method is that it requires no calibration standards.

■ ASSOCIATED CONTENT

Supporting Information. Supplemental 1, two approximations for quantifying droplet-induced dimers under some limiting conditions, (a) monomodal droplet size approximation and (b) bimodal droplet size approximation; supplemental 2,

derivations of formulas applied in two experimental approaches, (a) serial dilution and (b) changing droplet size, to obtain absolute concentrations of nanoparticles and protein using the two approximations described in supplemental 1; supplemental 3, further explanations of the droplet size distribution measurement. This material is available free of charge via the Internet at <http://pubs.acs.org>.

■ AUTHOR INFORMATION

Corresponding Author

*E-mail: mrz@umd.edu.

■ ACKNOWLEDGMENT

The identification of commercial equipment, instruments, or materials in this paper does not imply recommendation or endorsement by the University of Maryland or the National Institute of Standards and Technology.

■ REFERENCES

- (1) Daniel, M. C.; Astruc, D. *Chem. Rev.* **2004**, *104*, 293–346.
- (2) Haiss, W.; Thanh, N. T. K.; Aveyard, J.; Fernig, D. G. *Anal. Chem.* **2007**, *79*, 4215–4221.
- (3) Mulvaney, P. *Langmuir* **1996**, *12*, 788–800.
- (4) Khlebtsov, N. G.; Bogatyrev, V. A.; Dykman, L. A.; Melnikov, A. G. *J. Colloid Interface Sci.* **1996**, *180*, 436–445.
- (5) Yang, Y.; Matsubara, S.; Nogami, M.; Shi, J. *Mater. Sci. Eng., B* **2007**, *140*, 172–176.
- (6) Khlebtsov, N. G. *Anal. Chem.* **2008**, *80*, 6620–6625.
- (7) Kaufman, S. L.; Skogen, J. W.; Dorman, F. D.; Zarrin, F. *Anal. Chem.* **1996**, *68* (11), 1895–1904.
- (8) Bacher, G.; Szymanski, W. W.; Kaufman, S. L.; Zöllner, P.; Blaas, D.; Allmaier, G. N. *J. Mass Spectrom.* **2001**, *36*, 1038–1052.
- (9) Kim, S. H.; Zachariah, M. R. *Nanotechnology* **2005**, *16*, 2149–2152.
- (10) Kim, S. H.; Zachariah, M. R. *J. Phys. Chem. B* **2006**, *110*, 4555–4562.
- (11) Kim, S. H.; Zachariah, M. R. *Mater. Lett.* **2007**, *61*, 2079–2083.
- (12) Pease, L. F., III; Elliott, J. T.; Tsai, D.-H.; Zachariah, M. R.; Tarlov, M. J. *Biotechnol. Bioeng.* **2008**, *101* (6), 1214–1222.
- (13) Light-Wahl, K. J.; Winger, B. E.; Smith, R. D. *J. Am. Chem. Soc.* **1993**, *115*, 5869–5870.
- (14) Light-Wahl, K. J.; Schwartz, B. L.; Smith, R. D. *J. Am. Chem. Soc.* **1994**, *116*, 5271–5278.
- (15) Ayed, A.; Krutchinsky, A. N.; Ens, W.; Standing, K. G.; Duckworth, H. W. *Rapid Commun. Mass Spectrom.* **1998**, *12*, 339–344.
- (16) Nettleton, E. J.; Tito, P.; Sunde, M.; Bouchard, M.; Dobson, C. M.; Robinson, C. V. *Biophys. J.* **2000**, *79*, 1053–1065.
- (17) Lane, L. A.; Ruotolo, B. T.; Robinson, C. V.; Favrin, G.; Benesch, J. L. P. *Int. J. Mass Spectrom.* **2009**, *283*, 169–177.

- (18) Loo, R. R. O.; Dales, N.; Andrews, P. C. *Protein Sci.* **1994**, *3*, 1975–1983.
- (19) Cech, N. B.; Enke, C. G. *Mass Spectrom. Rev.* **2001**, *20*, 362–387.
- (20) Hogan, C. J.; Biswas, P. J. *Am. Soc. Mass. Spectrom.* **2008**, *19*, 1098–1107.
- (21) Li, M.; Guha, S.; Zangmeister, R.; Tarlov, M. J.; Zachariah, M. R. *Aerosol Sci. Technol.* **2011**, *45* (7), 849–860.
- (22) Tsai, D.-H.; Zangmeister, R. A.; Pease, L. F., III; Tarlov, M. J.; Zachariah, M. R. *Langmuir* **2008**, *24*, 8483–8490.
- (23) TSI model 3480 electrospray aerosol generator menu, TSI Inc., Shoreview, MN.
- (24) Hinds, W. C. *Aerosol Technology: Properties, Behavior, and Measurement of Airborne Particles*, 2nd ed.; Wiley: New York, 1999; Chapter 15.
- (25) Chen, D.-R.; Pui, D. Y. H.; Kaufman, S. L. *J. Aerosol Sci.* **1995**, *6*, 963–977.
- (26) Kebarle, P.; Tang, L. *Anal. Chem.* **1993**, *65* (22), 972–986.
- (27) Gaskell, S. J. *J. Mass Spectrom.* **1997**, *32*, 677–688.
- (28) Fernandez de la Mora, J. *Anal. Chim. Acta* **2000**, *406* (1), 93–104.
- (29) Lewis, K. C.; Dohmeier, D. M.; Jorgenson, J. W. *Anal. Chem.* **1994**, *66*, 2285–2292.